Article ID: 1003－6326(2004)03－0631－06

Operation optimization of concentrate burner in copper flash smelting furnace①

CHEN Hong-rong(陈红荣)[1], MEI Chi(梅 炽)[1], XIE Kai(谢 锴)[1], LI Xing-fen(李欣锋)[1],
ZHOU Jun(周 俊)[2], WANG Xiao-hua(王晓华)[2], GE Ze-lin(葛则令)[2]
(1. Institute of Simulation and Optimization of Pyro-installation,
Central South University, Changsha 410083, China;
2. Jinlong Copper Corporation, Tongling 244000, China)

Abstract: The software that simulates the flow, temperature, concentration and the heat generation field in the Outkumpu flash smelting furnace, was developed by a numerical method of the particle-gas flow together with some chemical reaction models. Many typical operating conditions were chosen for simulation in order to obtain the effect of the distribution air, process air, central oxygen and the oil-burner position etc. The concepts about optimum operation, 3C(concentration of high temperature, high oxygen and laden concentrate particles), are concluded from these simulated results, which have been checked primarily by operational experiments.

Key words: numerical simulation; flash smelting furnace; optimum operation; copper smelting
CLC number: TF 811 **Document code:** A

1 INTRODUCTION

The sulfuric concentrate drops into the flash smelting furnace (FSF) with surrounding injected oxygen enrichment air. The flash smelting process becomes a favorable firing smelting technique since the reaction is tremendously fast and no additional heat is theoretically necessary. Because so many factors are associated with this process, it is impossible to describe this smelting process by only one variable, and the mathematical models describing this process show nonlinear and strong coupling.

Because the complexity and severity of the process, it's not easy to perform an experiment with satisfaction. In recent decades, the simulation technique on the FSF has been improved with the development of computer technology, and it has experienced the development from the beginning of 1980's by Themelis[1] and Sohn[2] to simple two-dimensional and then three-dimensional models[3-5]. Now, more and more researchers utilize the commercial fluid flow packages such as CFX, Phoenics to study this process[6-12].

Even though, most of the numerical researches on FSF are still on the specific simulations stage, consider more the methods and details of the fields, not the relationship between input (working conditions) and output (such as productivity, pollution indication), and they give no direct guidelines to the operations.

In this paper, the simulation models have been developed and the software for the smelting process in the FSF is proposed. With this software, we simulate various working conditions in order to give a direction of the operational optimization on the concentrate burner.

2 MATHEMATIC MODEL

2.1 General description

The gas-particle flow simulated in this paper is treated by an Euler-Lagrangian method, in which the equation group of the gas-phase is deduced in Euler method, and the particles motions are tracked by the Lagrangian method. The gas-phase and particles are coupled by a method called Particle Source In Cell (PSIC). This treatment includes following several models and methods.

1) Gas-phase turbulent flow: $k-\varepsilon$ model;

2) Oil and gaseous sulfur combustion: self-code + EBU (eddy break-up) model;

3) Thermal radiation: zone method;

4) Copper concentrate combustion: self-code.

2.2 Gas-phase model

The conservation equations of mass, moment and energy can be expressed as the same form when the common dependent variable Φ is used:

$$\frac{\partial(\rho\Phi)}{\partial\tau}+\nabla\cdot(\rho U\Phi-\Gamma_\Phi\nabla\Phi)=S_{U\Phi}+S_{P\Phi} \quad (1)$$

where ρ is the density of the gas-phase, Γ_Φ is the diffusive coefficient for variable Φ, $S_{U\Phi}$ and $S_{P\Phi}$ are the source terms from gas-phase and particles.

① **Received date:** 2003－07－02; **Accepted date:** 2003－10－09
Correspondence: CHEN Hong-rong, Tel: +86-731-8877409; E-mail: hrchen@mail.csu.edu.cn

2.3 Particle motion model

The motion of the particles in Lagrangian framework can be described as:

$$\frac{\delta \xi}{\delta \tau} = \boldsymbol{U}, \qquad m\frac{\mathrm{d}\boldsymbol{U}}{\mathrm{d}\tau} = \boldsymbol{F} \tag{2}$$

where ξ is the position of the moving particle in Lagrangian coordinate system, $\boldsymbol{F}$ is the total forces applied on the particle. Only Stokes drag force and the gravity are considered, because other forces are smaller.

2.4 Chemical reactions of particles

2.4.1 Procedures and features

The concentrate particle is a mixture of chalcopyrite and inert material such as silica flux. Although the mechanisms of the chemical reactions of the chalcopyrite are very complicated, the procedure can still be roughly divided into three phases for our convenience of numerical simulation, and they are shown in Table 1.

2.4.2 Reaction rate

The reaction process is considered as a diffusion controlled process, which means that the chemical kinetics rate is infinite when compared with the mass transfer rate of the reactants (or products), then, the rate is calculated with a convective mass transfer model only.

In the decomposition phase, the reaction rate is governed by the moving rate of the dissociated gas sulfur from particle to gas phase, and in the oxidation phase, governed by oxygen moving rate from gas-phase to particle. According to the theory of boundary layer and mass transfer, the reaction rate can be calculated by following equation:

$$\frac{\mathrm{d}M}{\mathrm{d}\tau} = -\pi d_{\mathrm{p}}\rho D Sh(m_{\mathrm{p}} - m) \tag{3}$$

where M is the mass of the constituent in particle; m_{p} and m are mass fractions in particle and gas, respectively; d_{p} is the particle diameter; D is the mass diffusivity in gas-phase; Sh denotes Sherwood number which is determined by the following empirical formula:

$$Sh = 2.0 + 0.6Re^{0.5}\left(\frac{\mu}{\rho D}\right)^{1/3} \tag{4}$$

where μ is the dynamic viscosity.

Reactions in the third phase are treated simply, because no collisions between particles are considered.

2.5 Particle heat balance

The heat balance of a single particle can be expressed as:

$$\sum(m_i c_{pi})\frac{\mathrm{d}T}{\mathrm{d}\tau} = Q_{\mathrm{conv}} + Q_{\mathrm{rad}} + Q_{\mathrm{re}} \tag{5}$$

where i represents the different components of the particle; c_p is the specific heat capacity; Q_{conv} and Q_{rad} are the heat transferred by convection and thermal radiation between the particle and surrounding gas, respectively; Q_{re} is the heat released (or absorbed) by the chemical reaction which is determined by the particular reaction.

By the knowledge of heat transfer, the heat transferred by convection and thermal radiation will be

$$\left.\begin{aligned} Q_{\mathrm{conv}} &= \pi d\lambda Nu(T_{\mathrm{g}} - T) \\ Q_{\mathrm{rad}} &= \pi d^2 \varepsilon' \sigma(\varepsilon_{\mathrm{g}} T_{\mathrm{g}}^4 - \alpha_{\mathrm{g}} T^4) \end{aligned}\right\} \tag{6}$$

where $Nu = 2.0 + 0.6Re^{0.5}\left(\mu\frac{c_p}{\lambda}\right)^{1/3}$; λ is the thermal conductivity of the gas phase; ε_{g} and α_{g} are the emissivity and absorptivity of the gas phase; T_{g} and T are the temperature of gas-phase and particle, respectively; ε' is the effective emissivity of the particle.

The "copper FSF simulator" is then integrated by above models and the commercial fluid flow package CFX4.3 in which the user FORTRAN modules have been developed.

3 SIMULATION RESULTS AND DISCUSSION

3.1 Physical model of simulated FSF

Table 1 Reactions description

Phase	Feature	Position	Reaction equation
Thermal decomposition	Endothermic, sulfur dissociation	Particle	$5CuFeS_2 = Cu_5FeS_4 + 4FeS + 2S(g)$
	Exothermal	Gas-phase	$S(g) + O_2 = SO_2$
Oxidation	Exothermal, FeS under-oxidation	Particle surface	$2Cu_5FeS_4 + O_2 = 5Cu_2S + 2FeS + 3SO_2$
	Exothermal, FeS over-oxidation	Particle surface	$3FeS + 5O_2 = Fe_3O_4 + 3SO_2$
Collision, melting, and mergence together	Fe_3O_4 reduction	Inter-particle	$FeS + 3Fe_3O_4 = 10FeO + SO_2$
	Slag forming	Molten particle	$2FeO + SiO_2 = 2FeO \cdot SiO_2$
	Matte forming	Molten particle	$Cu_2S + FeS = Cu_2S \cdot FeS$

The ratio of FeO to FeS is determined from matte grade.

The simulated domain of FSF includes the reaction shaft and the settler. The reaction shaft of the Jinlong Corporation is 5 m in diameter and 6. 64 m in height. The concentrate burner consists of inner and outer air chambers, which can be opened up or shut down separately for regulation of the process air. The cross-section areas of the inner and outer air chambers on the entrance are 0. 027 5 m^2 and 0. 041 4 m^2. There is a cylindrical feed chute inside the inner air chamber for the concentrate particle dropping down into the reacting shaft, with a distribution air cylindrical pipe and then a central oxygen pipe enclosed in it. The feed mixture drops down from two opposite sides into the feed chute, disperses first along the cone surface on the bottom of the chute in a conic surface shape, then, disperses more by the distribution air, which blows out from the holes on the circumference of the cone bottom. On the roof of the reaction shaft, 1. 4 m departed from center, there are three oil burners uniformly installed along the circumference direction in order to compensate for the insufficient heat.

The whole structure of the FSF in the simulation should be simplified for deduction of the computing time, which is shown in Fig. 1. The concentrate burner locates on the top center of the reaction shaft and the details are shown in Fig. 2.

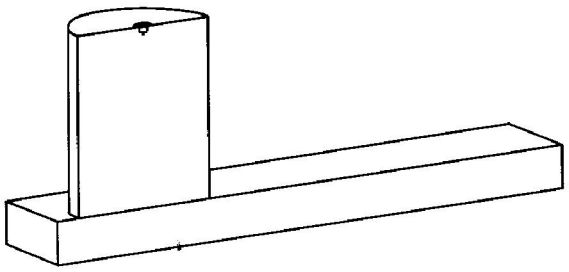

Fig. 1 Half structure of copper FSF

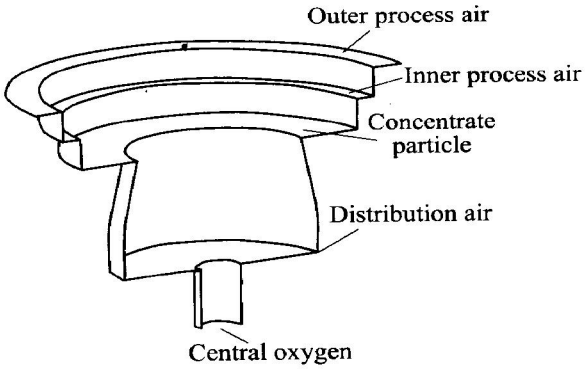

Fig. 2 Inlet of concentrate burner

3. 2 Simulated working conditions

In order to understand the effect of single-variable better, the simulations are arranged in a way that only the variable considered is set for different values and other variables are fixed. The speed of distribution air, the percentage of central oxygen in total oxygen, and the enrichment rate of the process air are main regarded single-variables. The predicted conditions are listed in Table 2. The other parameters for all predicted conditions are listed in Table 3.

3. 3 Results and discussion

The simulation results show the distribution of the velocity, temperature, concentration and the heat generation in details. The key parameters are the highest temperatures in gas-phase and particles, the mean temperature of the gas and the cone radius of the dropped particles (DP) on the slag surface. The results are summarized in Table 4.

Table 2 Simulated working conditions

No.	Oil consumption per ton feed mixture/ kg	Central oxygen/ %	Distribution air speed/ ($m \cdot s^{-1}$)	Process air enrichment/ %
1	13. 65	6	150	55
2	13. 65	6	160	55
3	13. 65	6	170	55
4	13. 65	6	180	55
5	13. 65	6	190	55
6	13. 65	6	200	55
7	13. 65	8	180	55
8	13. 65	10	180	55
9	13. 65	6	180	62
10	13. 73	11	130	55
11	13. 02	6	130	55

Table 3 Other related working conditions

Fe/ SiO_2 (Slag)	S/ Cu	Matte grade/ %	Matte temperature/ ℃	Slag temperature/ ℃
1. 15	1. 01	58	1 210	1 240

Table 4 Results summary

No.	Gas-phase		Particle highest temperature/ K	Radius of DP/ m
	Highest temperature/ K	Mean temperature/ K		
1	1 905	1 676	1 838	1. 50
2	1 905	1 676	1 838	1. 60
3	1 905	1 676	1 838	1. 65
4	1 905	1 676	1 838	1. 70
5	1 905	1 676	1 838	1. 72
6	1 905	1 676	1 838	N/ A
7	1 910	1 676	1 838	N/ A
8	2 148	1 676	1 838	N/ A
9	1 930	1 725	1 816	1. 70
10	2 121	1 676	1 880	1. 50
11	2 840	1 710	2 124	1. 50

The effect of distribution air can be seen from No. 1 - 6 of the Table 4. This table shows that the higher the speed of the distribution air is, the larger the radius of the DP is. It means that the particle is more dispersed when the speed of the distribution air is higher. Temperature values in this table show that they have no relationship with speed of distribution air. Therefore, higher speed of the distribution air is not necessary.

The results of No. 4, 7 and 8 show the effect of the central oxygen. Because the highest temperature in gas-phase appears always on the interface of particles and central oxygen, the larger one corresponds to the larger oxygen content, then the higher central oxygen content benefits the rise of the highest temperature in gas-phase. The average temperatures in the gas-phase have no relationship with central oxygen content, because the central oxygen occupies small percentage of all oxygen supplied (< 10%).

The effect of the process air enrichment is shown in the comparison of No. 4 and 9. The comparison tells us that the overall temperature and the highest temperature of gas-phase are increased, but the highest temperature of particles decreases somewhat, with the increase of the process air enrichment. The reason is that, on one hand the increasing process air enrichment helps the sulfur combustion that happens in the gas-phase, and then raises the temperature of the gas; on the other hand, the more combustion needs more sulfur dissociation which results in heat absorption and temperature drops of the particles.

For obtaining the optimum principle of operating parameters, the analysis is necessary to combine the optimum environment in different phase of the reaction process. According to the phase division in Table 1, the optimum environment conditions are summarized in Table 5.

Table 5 Optimum environment conditions for smelting process

Decomposition	Oxidation	Inter-particles reaction, slag, congregation
High temperature	High oxygen concentration	High particle concentration and high inter-particle collisions

The concentration of the particles is the first optimum operation suggestion, which results from the calculation of single-variable (distribution air) effect and the above optimum environments. The proper centralization of the particles will ensure most frequent collision between particles when chemical reaction takes place. This is beneficial to oxygen transfer among particles, slag formation, particles merging, particle enlarging, and particles falling. This makes it possible for higher matte grade and lower dust rate.

The concentration of the oxygen is the second optimum operation suggestion. It is obtained by combination of the effect of the process air enrichment, central oxygen, and the optimum environments shown in Table 5. More oxygen is helpful for combustion, especially oxidation reaction of the particles. But the oxygen is limited in actual operation by many factors such as the oxygen making ability and the speed rate, and it cannot be supplied with sufficient way as we like. Too much oxygen will make unnecessary waste, and the only way we can do is increasing the oxygen consuming-rate in the FSF. The distribution of the oxygen concentration in FSF for working condition No. 5 in Table 3 is shown in Fig. 3, and the other working conditions are similar.

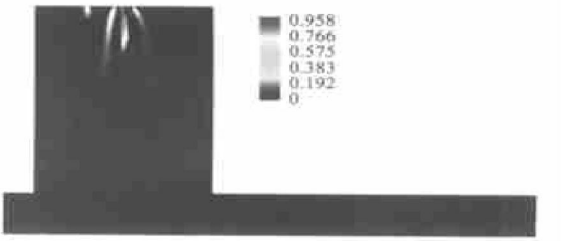

Fig. 3 No. 5 O_2 concentration distribution

It can be seen from Table 1 that the smelting process begins from the decomposition phase of the sulfuric concentrate particles. In order to make the decomposition go smoothly, the particle must absorb sufficient heat from surrounding with heat convection and thermal radiation, and its temperature must rise rapidly to the ignition temperature. The oil burners added are used for raising the particle temperature, so the heat should be concentrated and located on the entrance nearby. Theoretically, the third conclusion of the optimum operation, the high temperature region concentration, is formed from these ideas. In order to investigate this effect, the oil burner is moved from the circumference to the axis center with a working condition No. 11 listed in Table 3, and the temperature distribution is shown in Fig. 4. It shows clearly that the kernel of the high temperature ($T > 1\ 650$ K) is concentrated on the axis-nearby space.

It is concluded from above analysis that the intensive smelting benefits from the concentration of temperature, oxygen and the particles (3C). According to this guideline, we designed No. 10 and No. 11 working conditions. The above conclusions have been proven with the dust rate analysis from the particle tracks. In Fig. 5, four different working conditions are compared, where (a) is used as a comparison basis, (b) represents a higher process air enrichment, (c) gives

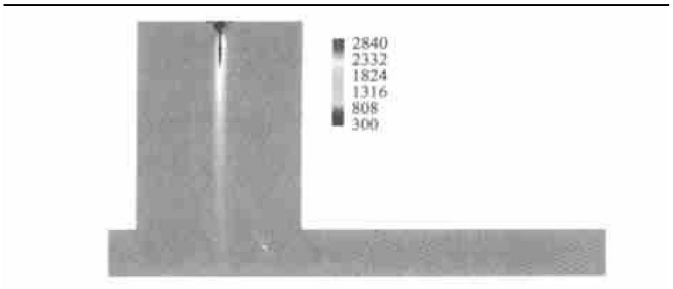

Fig. 4 No. 11 temperature distribution

higher central oxygen and lower distribution air velocity, and (d) has a lower distribution air velocity and oil burner is moved from outer circumference to axis.

The dust rate can associate with the particle numbers on the outlet of the settler. The more the particle flows there are, the higher the dust rate is. Fig. 5 shows that the dust rate is decreased from (a) to (d). It means that the higher process air enrichment will decrease the dust rate, the higher central oxygen and lower speed rate of the distribution air decrease more, and putting oil burner to axis instead of outer circumference and lower speed rate of the distribution air decrease most.

4 ON-SITE MEASUREMENTS AND OPERATION TESTS

Because of the severe, complicated on-site conditions, only temperatures are measured as a proof of the simulation. The temperature distribution was measured with both the special making double platinum-rhodium thermocouples and an infrared radiation pyrometer. The thermocouple is covered with a corundum jacket, which is inserted from roof into the FSF. Because the thermocouple has only 3m long, and the other locations far from this distance can only be measured with the infrared radiation pyrometer. The differences between these measured data and calculated ones are very small, which are shown in Table 6, and the changing trends along the height are nearly the same for both.

Table 6 Comparison of measured temperature and calculated temperature

Distance from roof/ m	Measured temperature/ K	Calculated temperature/ K
0. 22	1 608	1 613
0. 72	1 610	1 614
1. 52	1 615	1 616
3. 42	1 621	1 617
4. 85	1 627	1 618
5. 56	1 628	1 620

Jinlong Copper Corporation made the preliminary operation tests according to the '3C' operating principles, which show that when the feed mixture increases by 15%, the oil consumption in the reaction shaft decreases from original 20 kg to 13. 7 kg per ton feed mixture, the dust rate drops from 6. 5% to 5. 5%, and other indexes are better than before.

5 CONCLUSIONS

1) The simulation software "FSF numerical reactor" was constructed on the platform of CFX 4. 3 by the self-coding models of sulfur particles decomposition, oxidation and the gaseous sulfur combustion. A set of simulation tests of different working conditions are made of this software. The simulated results of the "FSF numerical reactor" give nearly the real nature of the process, according to temperature measurement and the operation experiences.

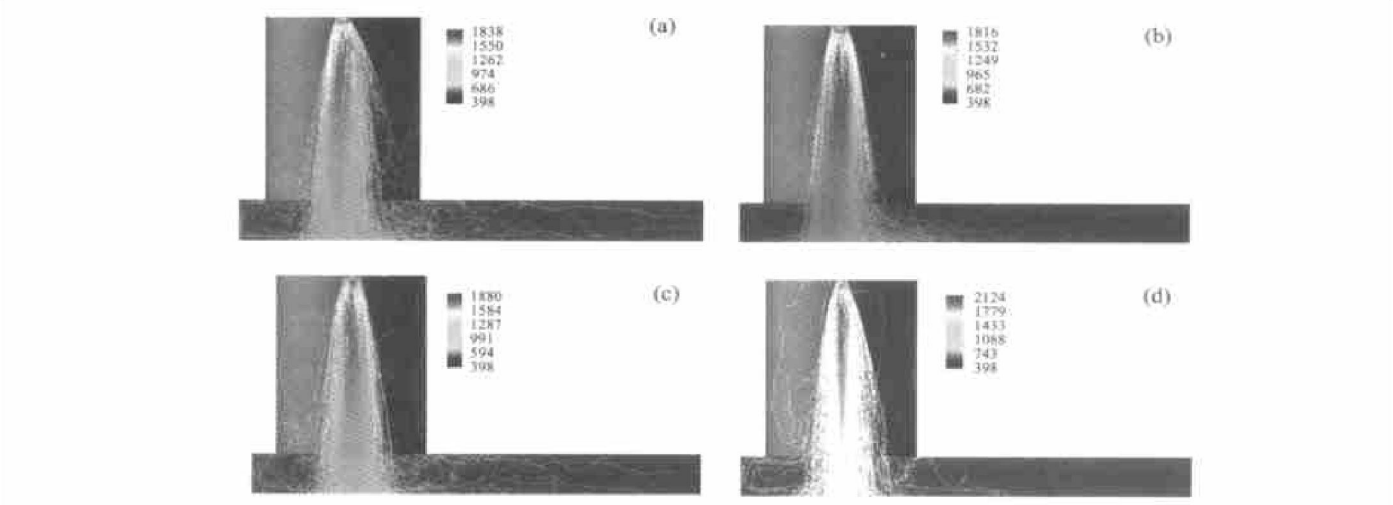

Fig. 5 Particle tracks and their temperature distributions
(a) —No. 4; (b) —No. 9; (c) —No. 10; (d) —No. 11

2) Through changing various single-variables and combining different multi-variables, how the working condition are affected by distribution air, central oxygen and the process air enrichment, is obtained, and it supplies a basis for further inductions.

3) The optimum operating 3C principle is summed up on the basis of the simulated test results. It means that the temperature, oxygen and concentrate particles must be centralized in order to intensify the smelting process, enhance the oxygen utilization, reduce the raw materials, dust and additional oil, and prolong the life of the reaction shaft. This principle is proven by a set of preliminary operating practices.

4) A frustum "high efficient reaction zone" is formed which locates under a certain distance from the concentrate burner, centers on the axis of the reaction shaft, according to the condition of 3C. With the concept of "high efficient reaction zone", the design is different from the traditional one, in which the average thermal strength based on the whole reaction shaft volume is used. The volume of "high efficient reaction zone" occupies only small part of the whole reaction shaft, and it reveals that the FSF still has very strong potentials to develop.

5) When the heat released by the concentrate particle reaction is not enough for the whole smelting process, putting the oil burner on the axis of the reaction shaft can use the oil released heat most, because most of the heat is added to the concentrate particles. In order to avoid the roof of the reaction shaft overheat, it still needs some explorative tests.

6) The above conclusions are all conceptual. Many quantitative relationships such as the range of every concentrations, the synthesis of the 3C, and the exact place of the "high efficient reaction zone" need more researches. We are working on these aspects for deeper understanding.

REFERENCES

[1] Jiao Q, Wu L, Themelis N J. Mathematical modeling of flash converting of copper matte[A]. Szekely J. Mathematical Modeling of Materials Processing Operations [C]. Warrendale: The Metallurgical Society, 1986. 835 - 858.

[2] Hahn Y B, Sohn H Y. Prediction of the behavior of the particle-laden gas jet as related to the flash-smelting process[A]. Szekely J. Mathematical Modeling of Materials Processing Operations [C]. Warrendale: The Metallurgical Society, 1986. 469 - 499.

[3] Hahn Y B, Sohn H Y. Mathematical modeling of sulfide flash smelting process: Part Ⅰ[J]. Met Trans B, 1990, 21B: 945 - 958.

[4] Hahn Y B, Sohn H Y. Mathematical modeling of sulfide flash smelting process: Part Ⅱ[J]. Met Trans B, 1990, 21B: 959 - 966.

[5] Seo K W, Sohn H Y. Mathematical modeling of sulfide flash smelting process: Part Ⅲ[J]. Met Trans B, 1991, 22B: 791 - 799.

[6] Ahokainen T, Jokilaakso A. Numerical simulation of the OUTOKUMPU flash smelting furnace reaction shaft[J]. Canadian Metallurgical Quarterly, 1998, 37: 275 - 283.

[7] LI Xing-feng, MEI Chi, ZHANG Wei-hua. Numerical simulation of fluid flow, heat transfer and combustion in the reaction shaft of copper flash furnace[A]. International Conference on Applied Computational Fluid Dynamics[C]. Beijing, 2000. 319 - 325.

[8] LI Xing-feng, MEI Chi, ZHANG Wei-hua, et al. Numerical simulations on copper flash smelting furnaces[J]. Journal of Central South University of Technology, 2001, 32(3): 262 - 266. (in Chinese)

[9] Jorgensen F R A, Eliot B J. Flash Furnace reacting shaft evaluation through simulation[A]. Misra V N. Int Conf on Extractive Met of Gold and Base Metals[C]. Kalgoorlie: Australasian Inst of Mining & Metallurgy Parkville, 1992. 387 - 394.

[10] Kon P T, Taylor R N. Mathematical modeling of heat transfer in flash smelting burners[A]. Misra V N. Int Conf on Extractive Met of Gold and Base Metals[C]. Kalgoorlie: Australasian Inst of Mining & Metallurgy Parkville, 1992. 407 - 411.

[11] Kon P T. Numerical simulation of two-phase flow in flash smelting burners[A]. Misra V N. Int Conf on Extractive Met of Gold and Base Metals [C]. Kalgoorlie: Australasian Inst of Mining & Metallurgy Parkville, 1992. 487 - 494.

[12] Kon P T, Jorgensen F R A. Modeling particulate flow and combustion in a flash smelter[A]. Mitchell P J. Australian Chem Eng Conf[C]. Perth: Australasian Inst of Mining & Metallurgy Parkville, 1994. 499 - 506.

(Edited by YUAN Sai-qian)